Food Hydrocolloids 149 (2024) 109597

Contents lists available at ScienceDirect

Food Hydrocolloids

journal homepage: www.elsevier.com/locate/foodhyd

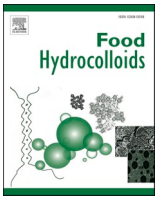

Protein bodies from hemp seeds: Isolation, microstructure and physicochemical characterisation

Duc Toan Do, Aiqian Ye, Harjinder Singh, Alejandra Acevedo-Fani *

Riddet Institute, Massey University, Private Bag 11 222, Palmerston North 4442, New Zealand

ARTICLE INFO

Keywords:
Hemp seeds
Protein bodies
Aleurone grains
Food microstructure
Protein stability
Edestin

ABSTRACT

Protein bodies are naturally occurring storage organelles in plant seeds. Although the microstructure of protein bodies has been studied, their physicochemical behaviour and stability under different environmental conditions remain poorly understood. In this study, hemp seed protein bodies (HPBs) were obtained using a sonication-assisted aqueous enzymatic extraction method. Then, their microstructures were characterised using various microscopic techniques. Next, the protein composition was determined using sodium dodecyl sulfate polyacrylamide gel electrophoresis (SDS–PAGE). Lastly, the influence of pH (2–13) on the colloidal stability and structural integrity of aqueous HPB dispersions was investigated. Detailed microscopic examination showed that the HPBs exhibited spherical shape with an average diameter of about 4.6 μm. The structure consisted of a protein crystalloid and several phytin globoids, all surrounded by a proteinaceous matrix and a single membrane. Globulin edestin was the most abundant storage protein in the HPBs as revealed by SDS–PAGE. The HPB dispersions exhibited excellent colloidal stability only at neutral pH as opposed to their aggregation and/or solubilisation at other pH levels tested. The HPBs also showed irreversible structural changes in response to pH variation. Specifically, little to no swelling of the particles was observed at pH 5 (around the isoelectric point (pI) of the hemp protein). However, when the pH shifted away from the pI, swelling, rupture and eventual dissolution of the particles were pronounced under both extreme acidic and alkaline conditions. These physicochemical behaviours make the HPBs an interesting pH-sensitive material for food applications, which will be explored in subsequent studies.

1. Introduction

The consumption of plant-based diets and alternative proteins are gaining in popularity thanks to their association with promoting environmental sustainability and human health (McClements & Grossmann, 2022). In plant-based foods, carbohydrates, proteins and lipids are deposited in small discrete storage organelles within plant cells. These organelles are termed starch granules, protein bodies (PBs) and oil bodies (OBs), respectively (Do, Singh, Oey, & Singh, 2018). Although the nature-assembled cellular structures, e.g., legume cotyledon cells (Do, Singh, Oey, & Singh, 2019), tuber parenchyma cells (Do, Singh, Oey, & Singh, 2020) and seed OBs (Garcia, Ma, Dave, & Acevedo-Fani, 2021), have been extensively characterised in recent years due to the intriguing relationship between their intact microstructures and their functionalities in food systems (Do et al., 2018), inadequate attention has been paid to the isolation and functional characterisation of PBs.

In seeds, amino acids are stored in the form of specific storage proteins and remain biochemically stable for long periods until they are required for germination. Storage proteins, thus, need to be protected against uncontrolled premature degradation, and this is achieved by their sequestration from the cytoplasm into specialised subcellular organelles called PBs or aleurone grains (Müntz, 1998). Intact PBs have been successfully isolated using differential centrifugation or density gradient centrifugation methods and involving aqueous or nonaqueous extraction media (Huang, 1985). Protein bodies are typically spherical organelles, and they vary in size among plant species and tissues, ranging from 0.1 to 25 μm in diameter. In terms of structure, a typical PB possesses an amorphous proteinaceous matrix surrounded by a single

Abbreviations: $d_{4,3}$, volume-weighted average diameter; CLSM, confocal laser scanning microscopy; HPB, hemp seed protein body; LM, light microscopy; MW, molecular weight; OB, oil body; PB, protein body; pI, isoelectric point; SDS–PAGE, sodium dodecyl sulfate polyacrylamide electrophoresis; SEM, scanning electron microcopy; TEM, transmission electron microscopy; β-ME, β-mercaptoethanol.

* Corresponding author.
E-mail address: a.acevedo-fani@massey.ac.nz (A. Acevedo-Fani).

https://doi.org/10.1016/j.foodhyd.2023.109597
Received 3 July 2023; Received in revised form 17 November 2023; Accepted 26 November 2023
Available online 2 December 2023
0268-005X/© 2023 The Authors. Published by Elsevier Ltd. This is an open access article under the CC BY license (http://creativecommons.org/licenses/by/4.0/).

membrane. Two types of inclusions, namely the crystalloid and the globoid, are often found embedded in the proteinaceous matrix. Depending on plant species, both of them can be present, and in some cases, only the globoid is present. The crystalloid consists mainly of globulin storage proteins, while the proteinaceous matrix is thought to be the location of other storage and non-storage proteins such as albumins, hydrolytic enzymes, protease inhibitors and lectins. Unlike the crystalloid, the globoid is not a proteinaceous inclusion, but is a storage site of cations and phytic acid (Pernollet, 1978).

Understanding of the microstructural and physicochemical properties of PBs is an important step towards improving the technological functionality and food utilisation of plant protein ingredients. We studied hemp seeds (*Cannabis sativa* L.) due to their growing use as a rich source of high-quality proteins for food applications. Unlike many other plant proteins, hemp proteins possess favorable characteristics such as adequate essential amino acids and excellent digestibility that enable them to have nutritional value comparable to egg white and soy protein (Shen, Gao, Fang, Rao, & Chen, 2021).

Protein bodies can be isolated from hemp seeds using density gradient centrifugation in a carbon tetrachloride-cottonseed oil mixture. The HPB is membrane-bound and contains a large crystalloid, globoids and other minor constituents. The crystalloid is composed primarily of globulin edestin which is the major hemp seed storage protein (Angelo, Yatsu, & Altschul, 1968). Although the microstructure of HPBs is well understood, little is known about their physicochemical behaviour in food-like environments. In this study, we reported for the first time efficient environmental-friendly extraction of PBs from hemp seeds using a sonication-assisted aqueous enzymatic method. We then provided the detailed characterisation of this new food material. The microstructures of PBs within hemp seed and after isolation were examined via various microscopy techniques. The physicochemical characteristics and stability of isolated HPBs in aqueous solutions at different pH were also evaluated.

2. Materials and methods

2.1. Materials

Commercially available dehulled whole hemp seeds, also known as hemp hearts, were purchased from Hemp Connect Ltd., Levin, New Zealand. The average nutritional composition of the hemp hearts provided by the seed producer was as follows: protein = 33 g/100 g, fat = 47 g/100 g, carbohydrate = 3.8 g/100 g and dietary fibre = 4.0 g/100 g. Viscozyme® L (Novozymes, Bagsværd, Denmark) was supplied by Azelis NZ Ltd. (Auckland, New Zealand). All other chemicals and reagents were of analytical grade. Milli-Q water from a Millipore Reference Milli-Q water purification system (Merck, Germany) was used to perform all experiments.

2.2. Isolation of hemp protein bodies

Intact PBs were isolated from hydrated hemp hearts using a sonication-assisted enzymatic method described by Al Loman, Callow, Islam, and Ju (2018). Modifications to the published method were made to improve the yield and purity of HPBs, based on a series of preliminary experiments (results not shown). Briefly, 30 g of hemp hearts were dispersed in 300 g of citrate buffer (50 mM, pH 5.0). To loosen the seed structure, the mixture was first sonicated for 5 min at a frequency of 200 W using an Ultrasonic Processor (Vibra Cell™ High Intensity Ultrasonic Processor Model 501, Sonics & Materials Inc, USA). Following the initial sonication, 0.75 mL of Viscozyme® L (a blend of various cell-wall-degrading enzymes) was added to initiate enzymatic hydrolysis of cell walls, leading to release of intracellular contents. Subsequently, the mixture was incubated in a water bath set at 50 °C with gentle magnetic agitation. The sonication treatment was then applied for 5 min at 200 W every 3 h during the first 12 h of extraction. A second dose (0.75 mL) of Viscozyme® L was added after 12 h and the mixture was left to incubate in the water bath for an additional 12 h. The pH was adjusted to 5.0 with 3 M HCl, if necessary, throughout the process. Following a total of 24 h of extraction, the enzymatic reaction was terminated by removing the mixture from the water bath. Afterwards, the resulting "milky" slurry was passed through 250 μm and 38 μm standard testing sieves (Endercotts, London, UK) to remove remaining hemp particles and hull residues. The filtrate, hereafter referred to as "hemp milk", was transferred into 50 mL centrifuge tubes and centrifuged at 3800×*g* for 30 min at room temperature (Heraeus Multifuge X3R, Thermo Scientific Inc, Germany). Following centrifugation, the top cream layer and the middle supernatant layer were carefully decanted by inverting the tubes. The HPB-rich pellet settled at the bottom of the tubes was then washed with absolute acetone at a wet-solid-to-solvent ratio of 1:10 (w/v) and recentrifuged at 3800×*g* for 20 min to remove OBs and free oil. This was immediately followed by washing of the pellet with pH-adjusted Milli-Q water at a wet-solid-to-water ratio of 1:10 (w/v) and pH ~ 5.0, then centrifugation again at 3800×*g* for 20 min to remove water-soluble proteins and sugars. The washed HPBs were freeze dried at −50 °C and <0.1 mbar for 24 h in a laboratory scale freeze dryer (Labconco, Kansas City, MO, USA). The PB powder was stored in a sealed container at room temperature until further analysis. To investigate the effect of sonication on the separation of cellular components, a control batch of hemp hearts was subjected to the extraction procedure as described above without any sonication treatments.

In addition, as an alternative to the mild enzymatic extraction, mechanical grinding was applied to hemp hearts in an attempt to recover intact PBs. Briefly, based on the method described by Lopez et al. (2021) with minor modifications, 100 g of hemp hearts were soaked in 300 mL of water for 20 h at 4 °C to allow seed hydration. The seed dispersion was then ground using a 1000-Watt hand-held blender (Brabantia BBEK1061, China) at speed setting "5" for 3 min to break the cell walls and release the intracellular contents. The resulting hemp slurry was filtered through cheesecloth to remove hull residues and cell wall materials. The filtrate was centrifuged at 3800×*g* for 30 min at room temperature to obtain a protein-rich sediment containing the PBs.

2.3. Microstructure

The microstructural characteristics of PBs within hemp seeds and after isolation were examined using light microscopy (LM), confocal laser scanning microscopy (CLSM), transmission electron microscopy (TEM) and scanning electron microcopy (SEM).

2.3.1. Light microscopy (LM)

To prepare samples for LM, aqueous dispersions of HPBs were mounted onto microscope slides and covered with glass coverslips. The samples were then viewed under an Olympus BX53 light microscope (Olympus, Tokyo, Japan) equipped with an oil-immersion objective at 100 × magnification in bright-field mode. Representative light micrographs were captured using an Olympus XC50 camera and processed using XIMEA CamTool 4.24 software (XIMEA GmbH, Münster, Germany).

2.3.2. Confocal laser scanning microscopy (CLSM)

The microstructures of the hemp milk and HPBs were studied using a confocal laser scanning microscope (Model Zeiss LSM900 with Airyscan 2, Carl Zeiss, Jena, Germany) equipped with a 63 × oil immersion objective. The samples were selectively stained with Nile Red (1 mg/mL in acetone) for neutral lipids and Fast Green FCF (1 mg/mL in Milli-Q water) for proteins. The stained samples were placed on concave microscope slides, covered with glass coverslips and viewed under the microscope. Nile Red was excited with an argon laser at 488 nm and the emitted fluorescent light was collected between 494 and 605 nm. Fast Green FCF was excited with a helium-neon laser at 633 nm and the emitted light was collected between 638 and 750 nm. Representative

confocal micrographs were captured using Zeiss ZEN 3.1 (Blue Edition) imaging software (Carl Zeiss, Germany) and processed using ImageJ software (National Institutes of Health, Bethesda, MD, USA).

2.3.3. Transmission electron microscopy (TEM)

For the examination of the hemp seed microstructure, hemp hearts were split into cotyledons that were fixed in modified Karnovsky's fixative (3% (v/v) gluteraldehyde and 2% (w/v) formaldehyde in 0.1 M phosphate buffer at pH 7.2) for at least 2 h. The fixed cotyledon tissues were washed 3 times in 0.1 M phosphate buffer at pH 7.2 for 10 min each, and then post fixed with 1% osmium tetroxide in the phosphate buffer for 1 h. The tissues were again washed 3 times as described above and dehydrated through a graded acetone series (25%, 50%, 75%, 95%, 100%) for 10–15 min at each concentration followed by two changes of 100% for 1 h each. The dehydrated tissues were embedded with a 50/50 resin/acetone mixture overnight which was then replaced with fresh 100% resin (Procure 812, ProSciTech Australia) for additional 8 h. Ultra-thin sections (70 nm thick) were cut from the resin blocks using a diamond knife (Diatome, Switzerland) and an ultramicrotome (Leica, Vienna, Austria), then mounted on copper grids using a Coat-Quick "G" pen (Daido Sangyo, Japan). The grids were stained with saturated uranyl acetate and lead citrate, with 50% ethanol and Milli-Q water washing steps included. The hemp cotyledon tissues were viewed using a FEI Tecnai G^2 Spirit BioTWIN transmission electron microscope (FEI Corp., Brno-Černovice, Czech Republic). Representative TEM micrographs were captured using a Veleta charge-coupled device (CCD) camera equipped with iTEM software (Olympus Soft Imaging Solutions GmbH, Münster, Germany).

For the microstructural examination of freshly isolated HPBs, they were first injected into freshly prepared 3% agarose gel tubes. The tubes were then fixed in 3% glutaraldehyde in 0.1 M sodium cacodylate buffer at pH 7.2 for at least 24 h. After fixation, the tubes were routinely processed for TEM by osmification, serial dehydration and embedding in resin before sectioning and viewing as described previously for hemp seeds.

2.3.4. Scanning electron microscopy (SEM)

Freeze dried powder samples were directly mounted on double-sided adhesive tapes on aluminium stubs, sputter coated with gold (SCD 050, Balzers, Liechtenstein), and viewed under a scanning electron microscope (FEI Quanta 200 FEI Electron Optics, Eindhoven, the Netherlands). Representative SEM micrographs were captured at 2 kV accelerating voltage and two magnifications of 1200× and 6000 × using the xT 3.0.7 microscope software (FEI Quanta, Eindhoven, the Netherlands).

2.4. Proximate analysis

The hemp milk and its three fractions obtained by centrifugation were analysed separately for moisture, crude protein, fat and carbohydrate. Moisture content was determined using vacuum oven drying method (AOAC 990.19, 990.20). Crude protein content was determined using Kjeldahl method (AOAC 991.20) with a nitrogen-to-protein conversion factor of 5.3 (Alonso-Esteban et al., 2022). For the determination of total fat content, given only a small quantity of samples available for testing, it was not practical to use the standard method of solvent extraction followed by gravimetric quantification of the extracted oil. Therefore, the total fat content was analysed by gas chromatography and expressed as fatty acid methyl esters (FAMEs) via the transesterification process according to the method described by Zhu, Ye, Verrier, and Singh (2013) with minor modifications. The FAME chromatogram was obtained and converted to the total fat percentage. Total carbohydrate content was determined using the colorimetric phenol-sulphuric acid method described by DuBois, Gilles, Hamilton, Rebers, and Smith (1956) and modified by Banskota, Tibbetts, Jones, Stefanova, and Behnke (2022). To ensure good reproducibility, all compositional analyses were performed in triplicate, and results were expressed on dry weight basis (dwb) as means ± standard deviations.

2.5. Sodium dodecyl sulfate–polyacrylamide gel electrophoresis (SDS–PAGE)

The protein profiles were evaluated by SDS–PAGE under both non-reducing and reducing conditions as per the method described by Manderson, Hardman, and Creamer (1998). Briefly, the hemp milk (M), supernatant (S), PB pellet (PBP) and washed HPBs (WPB) were mixed with SDS–PAGE sample buffer to a final protein concentration of 2 mg/mL. For the reducing conditions, the sample buffer was prepared by the addition of β-mercaptoethanol (β-ME) (5%, v/v). The reducing samples were heated at 95 °C for 10 min in a boiling water bath prior to loading. Aliquots (7 μL) of the samples were then loaded onto fresh glycine gels prepared in-house and run at a constant voltage of 150 V for approximately 90 min. After electrophoresis, the gels were stained in Coomassie brilliant blue solution (0.3% w/v) in 20% (v/v) isopropanol and 10% (v/v) glacial acetic acid and subsequently destained in 10% (v/v) isopropanol and 10% (v/v) glacial acetic. The destained gels were scanned using a molecular imager Gel Doc XR system (Bio-Rad Laboratories, Richmond, CA, USA).

2.6. Physicochemical characterisation

2.6.1. Particle size

The size distributions were measured in triplicate by static light scattering using a Mastersizer 2000 laser diffraction particle size analyser (Malvern Instruments Ltd., Worcestershire, UK). Samples were added into an automated small volume liquid dispersion unit (Hydro 2000S). The refractive indices of 1.45 and 1.33 were used for the proteins and the continuous phase (water), respectively. The particle size was reported as the volume-weighted average diameter ($d_{4,3}$, μm) using the following Eq. (1):

$$d_{4,3} = \sum \frac{n_i d_i^4}{n_i d_i^3} \quad (1)$$

where n_i is the number of particles with diameter of d_i.

2.6.2. Electrical surface charge of hemp protein bodies

The surface charge or zeta potential (ζ) of HPBs at different pH levels and ionic strength was measured using a Zetasizer Nano ZS (ZSU5800, Malvern Instruments Ltd., Malvern, UK), following the method described by Li and Xiong (2021). Aqueous suspensions of freshly isolated HPBs (10 mg/mL) were prepared with NaCl solutions at four ionic strength conditions (0, 0.01, 0.1 and 1 M NaCl) and seven pH levels (2.0–8.0) before being diluted to a final concentration of 0.1 mg/mL. The pH adjustments were carried out using appropriate concentrations of HCl or NaOH. The samples were injected into a folded capillary electrophoresis cell (DTS1070, Malvern Instruments Ltd., Malvern, UK) using a syringe. The ζ–potential of each sample was the mean averaged across at least 20 readings and measured in triplicate at 25 °C. The refractive indices of 1.45 and 1.33 were used for the proteins and the continuous phase (water), respectively. The ζ–potential values were calculated from the electrophoretic mobility of particles using the Smoluchowski approximation, according to Henry's law.

2.6.3. Effect of pH on stability of hemp protein bodies

Freshly prepared HPBs were dispersed in pH-adjusted Milli-Q water at a wet-solid-to-water ratio of 1:10 (w/w) and twelve pH levels (2–13). The pH adjustments were carried out using appropriate concentrations of HCl or NaOH (0.1–3 M). The PB dispersions were then mixed with magnetic stirrers at 300 rpm and 25 °C for 1 h. The particle size and the microstructure as a function of pH were evaluated using the methods previously described in Section 2.6.1 and 2.3.1, respectively.

3. Results and discussion

3.1. Microstructure of hemp seed

TEM examination of a thin section of hemp heart tissue showed the spatial organisation and morphology of two major organelles, the PBs and the OBs, inside the hemp seed (Fig. 1A). The hemp tissue consisted of cotyledon cells that were bound to each other by their surrounding cell walls (green arrows). Within each cell, the PBs (white arrows) could be easily distinguished from the electron-transparent OBs (red arrows) by their high electron density. The PBs were found to be sporadically distributed inside the cell with the numerous OBs filling the cytoplasmic space between them. At the microscopic level, the majority of these organelles had spherical shape with diameters of 1–4 μm and homogeneous appearance. Many of them with distorted shapes were noted as well, perhaps due to their dense packing within the cells and the organelles being pressed against each other. These findings are consistent with previous microscopic observations of hemp seed microstructure (Angelo et al., 1968; Garcia et al., 2021; Lee, Kim, & Kim, 2011; Lopez et al., 2021).

Closer inspection of an individual HPB at higher magnification revealed the finer details of its organisational structure. Fig. 1B indicated the presence of two distinct types of inclusions inside the PB, including one crystalloid and several spherical globoids. These appeared to be held together by a homogeneous proteinaceous matrix and enclosed by a membrane. Structurally, the globoids seemed to possess surrounding membranes and are the storage sites for seed phosphorous deposited as phytate salts (Prattley & Stanley, 1982). On the other hand, the crystalloid occupied a large volume of the HPB and is known to exhibit partly crystalline protein structure (Pernollet, 1978). There was also a clear absence of membrane surrounding the crystalloid. Similar TEM results have been reported earlier for PBs of hemp seeds (Angelo et al., 1968).

Previous studies have also clearly established the presence of two major components of the globoid, of which the electron-dense crystal is usually enclosed in the electron-transparent region. This region is termed the soft globoid and is presumably enveloped by a single outer membrane (Boatright & Kim, 2000; Lott & Buttrose, 1978; Lott, Larsen, & Darley, 1971; Varriano-Marston & DeFrancisco, 1984). Based on these reports, the soft globoids could easily be recognised within the HPB (blue arrows in Fig. 1B). They were often devoid of the electron-dense crystals and appeared to be extracted by the fixation procedure. It is known that the globoid crystals are brittle and are poorly penetrated by resin. They tend to shatter during the conventional TEM sample preparation and thus appear as cavities, oval or round in shape (Krishnan, 2008; Lott & Buttrose, 1978; Lott et al., 1971; Prattley & Stanley, 1982). Fig. 1B illustrates the existence of some electron-dense substances that appeared to be remnants of the globoid crystals inside a cavity (yellow arrow), all surrounded by the transparent area (soft globoid). It is possible that the globoid crystals could have fractured and subsequently detached from the hemp tissue during thin sectioning, leaving behind empty cavities, some of which may still contain weakly stained crystal fragments.

Furthermore, it is worth noting that while some HPBs contained two types of inclusions (Fig. 1B), some others lacked them completely or had only electron-dense crystalloids as clearly seen in Fig. 1A. The internal structures of seed PBs have previously been demonstrated to vary with their location within the tissue, and sometimes can vary from cell to cell within the same plane of section (Lott & Buttrose, 1978). However, one cannot rule out the preparative procedures for TEM as a possible source of these variations. Many factors pertaining to sample fixation and sectioning could alter the appearance and ultrastructural integrity of PBs and their sub-organelle compartments. These factors may include, but are not limited to, the type, concentration and osmolarity of buffers used for the fixatives, the fixation period and the post-fixation with osmium tetroxide (Boatright & Kim, 2000; Krishnan, 2008).

3.2. Isolation of hemp protein bodies

The aqueous enzymatic process applied to the hydrated hemp hearts induced hydrolysis of the cotyledon cell walls by Viscozyme® L, thereby enabling release of the intracellular organelles into the extraction medium and their subsequent separation by centrifugation (Fig. 2A). It could be assumed that the cell wall hydrolysis progressed radially inwards towards the core of the tissue in a layer-by-layer fashion, similar to a mechanism proposed by Al Loman et al. (2018) for the enzymatic separation of intact PBs and OBs from soybeans. In addition, these authors suggested that the use of sonication enhanced the process

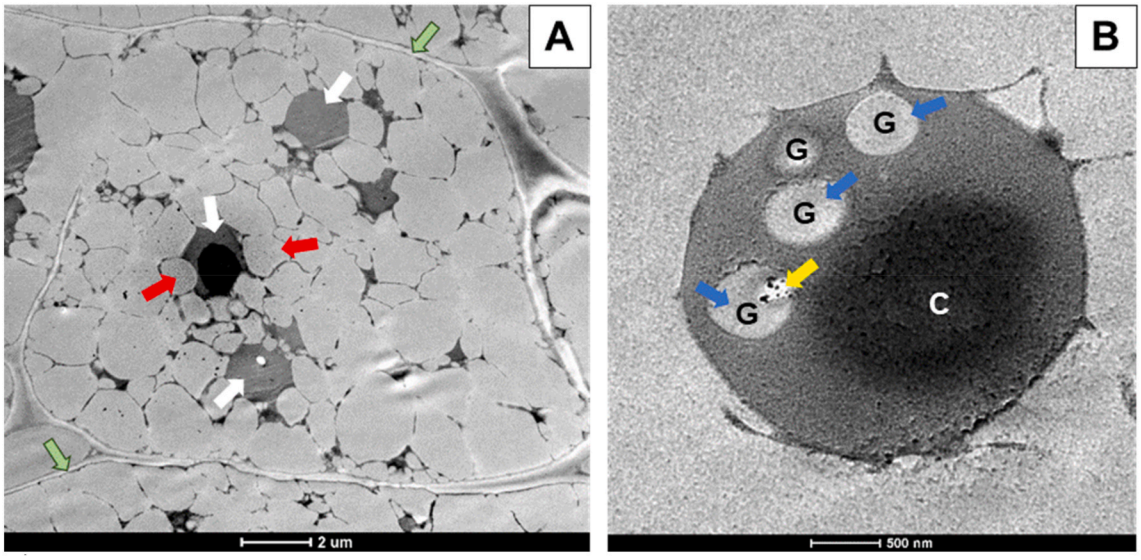

Fig. 1. (A) Representative Transmission Electron Microscopy (TEM) image of a cross-section of hemp heart tissue. Scale bar = 2 μm. Green arrows indicate the presence of cotyledon cell walls (CWs). White arrows indicate hemp protein bodies (HPBs) while red arrows indicate oil bodies (OBs). (B) Representative TEM image of a HPB showing two distinct types of inclusions: the crystalloid (C) and the globoid (G). Scale bar = 500 nm. The globoids consist of crystals surrounded by transparent areas as indicated by blue arrows. The globoid crystals shatter upon thin sectioning of the hemp tissue, leaving behind a cavity and some electron-dense fragments (yellow arrow).

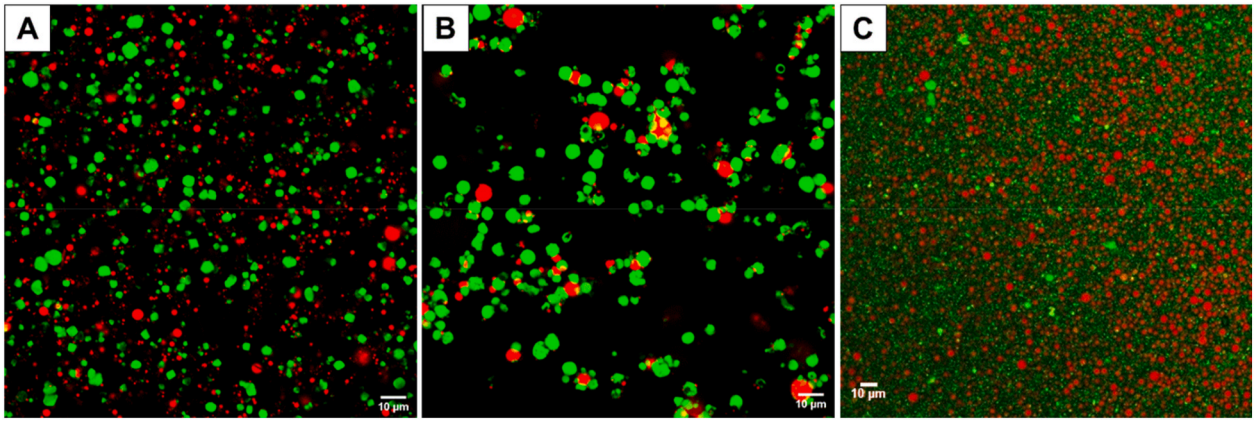

Fig. 2. Effects of aqueous extraction method on recovery of HPBs from hemp hearts. The representative Confocal Laser Scanning Microscopy (CLSM) image in panel (A) was from the HPB-rich pellet obtained by centrifugation of the hemp milk following the sonication-assisted enzymatic processing of hemp hearts. This pellet consisted mainly of individually dispersed PBs (green) and OBs (red). Without the aid of the sonication treatment, large PB–OB clusters were observed in the panel (B) image, indicating a lack of separation of these two subcellular organelles. The CLSM image in panel (C) was from the protein-rich sediment obtained through the grinding of hemp hearts in water, followed by the filtration and centrifugation of the resulting hemp slurry. This sediment consisted mainly of OBs (red), proteins and possibly cell wall debris (green). Very few intact spherical-shaped PBs could be seen. The oil (in red) and the protein (in green) were stained with Nile Red and Fast Green FCF, respectively. Scale bar = 10 μm.

performance. In the present study, the sonication prior to the enzyme processing may have led to break-up of the hemp hearts into smaller particles and loosening of the cotyledon cell structure. During the enzyme processing, the periodic application of sonication (every 3 h during the first 12 h) could facilitate dislodging of the organelles from the cellular matrix in the outermost layers of the hemp particles and, at the same time, could expose the cell walls in the inner layers for hydrolysis. Without the aid of sonication, some HPBs remained adhered to OBs, forming PB–OB aggregates, as demonstrated in Fig. 2B. Hence, the sonication treatment proved effective in breaking the large aggregates into individually dispersed particles, as shown in Fig. 2A. Also noticeable in this figure is that the enzymatic extraction appeared to preserve the intact structure of HPBs while minimising their potential contamination with cell wall debris during subsequent purification steps. When a conventional protein extraction method involving grinding (homogenisation) of hemp hearts was also employed to release subcellular components (method detailed in section 2.2), the recovery of intact HPBs was relatively low. Compared with the enzymatic processing, the

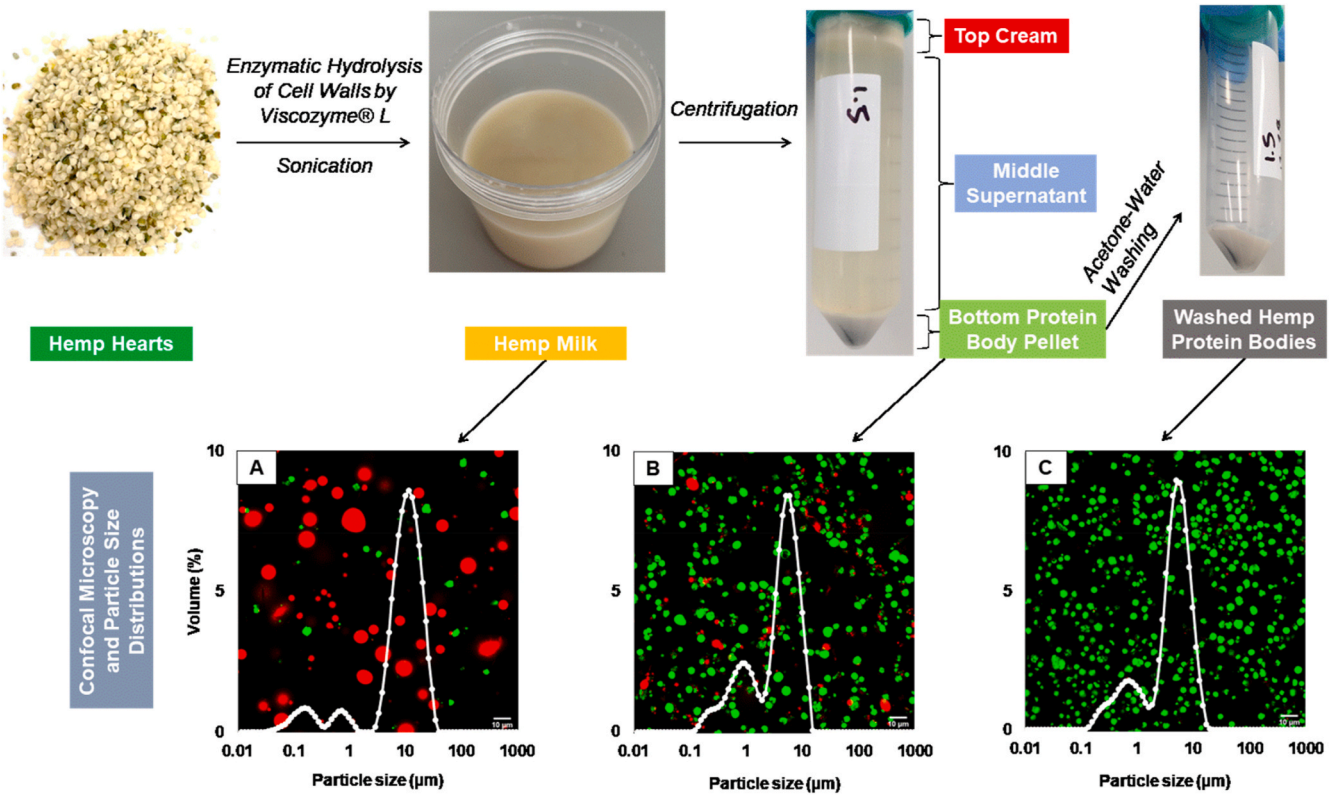

Fig. 3. Characterization of hemp materials obtained along the sonication-assisted aqueous enzymatic extraction process: Representative CLSM images (scale bar = 10 μm) and particle size distributions of hemp milk (A), PB pellet (B) and washed HPBs (C). The oil (in red) and the protein (in green) were stained with Nile Red and Fast Green FCF, respectively.

intensive grinding was found to induce greater degree of PB disruption and contamination with cell wall materials (Fig. 2C).

It has been well documented that it is difficult to isolate pure PBs with all components intact since they are readily destroyed during homogenisation of seed tissues (Elpidina, Dunaevsky, & Belozersky, 1990). Protein bodies are also unstable in the aqueous isolation medium. Buffering the medium to pH 4.5–5.0, around the pI of the protein, confers some stabilising effect. A low ionic strength buffer is also critical to maintain PB integrity since a high ionic strength can solubilise most of the protein. Further, PBs can easily be contaminated with cellular components such as starch granules, OBs and cell wall fragments, which renders separation challenging because of their similar physical properties, such as particle size range (Donhowe & Peterson, 1983; Elpidina et al., 1990; Tombs, 1967). Considering these difficulties, we chose the mild enzymatic method of cell wall hydrolysis at pH 5.0 and low ionic strength in order to stabilise and purify HPBs.

3.3. Characterisation of hemp materials obtained during the isolation process

As illustrated in Fig. 3, the sonication-assisted enzymatic hydrolysis of cell walls effectively reduced the hydrated hemp hearts to hemp milk. Subsequent centrifugation of the hemp milk allowed its separation into three distinct layers, i.e., the top cream, the middle supernatant and the bottom PB pellet. Further purification of the PB pellet was achieved by washing it successively with acetone and water, whereby residues of oil and water-soluble proteins/sugars were removed, respectively. Physicochemical and microscopic analyses were then carried out in order to identify the components present in the hemp milk and each of its three fractions obtained by centrifugation.

The protein, fat and carbohydrate distributions (on a dry weight basis) in the studied samples are given in Table 1. The hemp milk consisted predominantly of protein (29.09 ± 0.15%) and fat (45.12 ± 0.76%) with a small carbohydrate content (3.53 ± 0.13%). The CLSM image of the freshly extracted hemp milk (Fig. 3A) showed a dispersion containing PBs, OBs and free oil droplets. Some OBs could have been broken during the extraction procedure and coalesced to form larger oil droplets. The particle size distribution of the hemp milk determined by static light scattering was polydisperse with a volume-weighted average diameter ($d_{4,3}$) of 10.7 ± 1.3 μm. The centrifugation of the hemp milk resulted in the top cream layer enriched with fat (97.37 ± 1.20%), the middle supernatant layer enriched with soluble protein (21.15 ± 0.15%) and hydrolysed carbohydrates (78.21 ± 1.79%), and the bottom PB pellet layer enriched with protein (80.70 ± 0.71%). The sequential acetone-water washing of the PB pellet further enriched this fraction with protein (90.79 ± 0.57%), while simultaneously reducing its fat (8.73 ± 0.63%) and carbohydrate (0.88 ± 0.02%) contents to 0.95 ± 0.02% and 0.28 ± 0.01%, respectively. The CSLM image of the PB pellet (Fig. 3B) showed the presence of PBs (both intact and broken), OBs and free oil droplets, while that of the washed HPBs (Fig. 3C) showed mostly individually dispersed PBs and very little oil, thus confirming the compositional results. The $d_{4,3}$ and size distribution of the PB pellet dispersed in water at neutral pH were determined to be 4.4 ± 0.2 μm and in the range from 0.1 to 20 μm, respectively. These values remained relatively similar after the two washing steps. The $d_{4,3}$ and size distribution of the washed HPBs dispersed in water at neutral pH were 4.6 ± 0.0 μm and in the range from 0.1 to 20 μm, respectively, indicating that the PB pellet was composed of predominantly HPBs. These findings may also be suggestive of a similar particle size between the washed-off OBs and HPBs. According to previous reports, the size distribution of hemp OBs ranged from 0.3 to 20 μm with $d_{4,3}$ ~2.3–4.9 μm (Garcia et al., 2021; Lopez et al., 2021). In comparison, the size of HPBs were in the range between 1.3 and 20 μm in diameter with $d_{4,3}$ ~4.1 ± 0.3 μm (Angelo et al., 1968; Lopez et al., 2021), in agreement with the data produced in the present work.

Looking closely at Fig. 3C, we may easily identify two particle size fractions of the washed HPBs: 0.1–2 μm and 2–20 μm. Generally, considerable destruction or contraction of large PBs (e.g., >10 μm in diameter) is almost certain in aqueous systems, even under mild homogenisation conditions, resulting in smaller size of isolated PBs compared to those found in intact seed tissues (Donhowe & Peterson, 1983; Elpidina et al., 1990; Lee, Kim, & Yang, 1983). Specifically, the intact PBs were mostly concentrated in the coarse fraction (2–20 μm) that dominated the distribution with a sharp peak around 5 μm. The fine fraction (0.1–2 μm) possibly contained many small proteinaceous granules released from disrupted PBs.

In addition, under the extraction conditions (pH 5.0 and 50 °C) used, the freshly prepared HPBs (Fig. 3C) were observed to be largely unaggregated. Similarly, Al Loman et al. (2018) noted well-dispersed PBs freshly extracted from soybeans at pH 4.8 and 50 °C. The evidence again confirms the effectiveness of the sonication treatment for dissociation and dispersion of HPBs in the aqueous extraction medium. Moreover, the use of water as a dispersant at neutral pH for Mastersizer and microscopic analysis could disrupt flocs formed at pH 5.0 and keep the particles apart in response to pH-induced modifications of their surface charges. This pH effect will be demonstrated in the later sections.

Table 1
Percentage weight distribution of protein, fat and carbohydrate in hemp milk and each of its three fractions obtained by centrifugation*.

Hemp Samples	Protein (%)	Fat (%)	Carbohydrate (%)
Hemp Milk	29.09 ± 0.15^{c}	45.12 ± 0.76^{b}	3.53 ± 0.13^{b}
Top Cream	2.92 ± 0.04^{e}	97.37 ± 1.20^{a}	0.40 ± 0.03^{d}
Middle Supernatant	21.15 ± 0.15^{d}	0.41 ± 0.02^{e}	78.21 ± 1.79^{a}
Bottom Protein Body Pellet	80.70 ± 0.71^{b}	8.73 ± 0.63^{c}	0.88 ± 0.02^{c}
Washed Hemp Protein Bodies	90.79 ± 0.57^{a}	0.95 ± 0.02^{d}	0.28 ± 0.01^{e}

*All data were reported on a dry weight basis. Values were the means and standard deviations of triplicate measurements on each sample. Letters (a–e) indicate significant difference ($P < 0.05$) within the same column.

3.4. Microstructure of isolated hemp protein bodies

Following the extraction, the ultrastructural characteristics of the isolated HPBs were studied using a combination of LM, TEM and SEM. Micrographs obtained from the different microscopy techniques (Fig. 4) revealed different aspects of the PB morphology. Fig. 4A displays the light micrograph of the freshly isolated HPBs dispersed in water. The particles were identifiable as free PBs by their size, shape and structure. They tended to exist as spherical-shaped discrete bodies with the diameters ranging from 1 to 5 μm, though, some had clumped together, forming large aggregates. Most of the HPBs appeared to remain morphologically intact after the isolation process as evidenced by the presence of well-defined membranes. Further probing of an enlarged PB under LM (Fig. 4A, inset, upper right corner) enabled visualisation of the structure in much greater detail. The internal organisation consisted of areas of dark material arranged in concentric rings. These concentric patterns seemed to correlate to those observed by TEM in previous studies. Several researchers have reported the alternative arrangement of electron-dense (dark-staining) and electron-thin (light-staining) regions within the PB matrix from several plant species, which conforms to the internal concentric ring structure (Adams & Novellie, 1975; Lending, Kriz, Larkins, & Bracker, 1988; Mitsuda, Murakami, Kusano, & Yasumoto, 1969).

The ultrastructural features of the isolated HPBs were also examined using TEM. As seen in Fig. 4B, the sample was slightly contaminated with OBs and cell debris. A large number of PBs had apparently survived

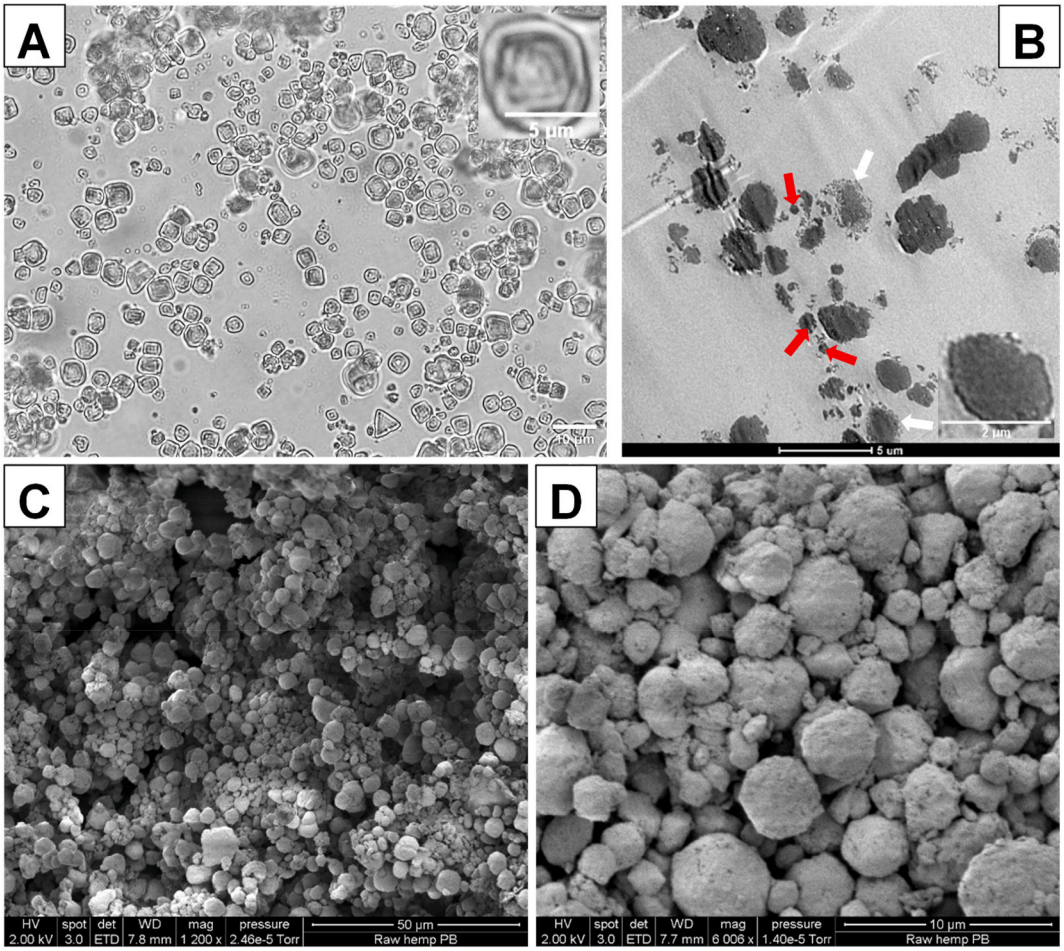

Fig. 4. Representative microstructural images of isolated HPBs captured by various microscopy tools. (A) LM micrograph (scale bar = 10 μm) in bright-field mode showing PBs with intact membranes. A higher magnification (inset) clearly revealed the internal structure consisting of areas of dark material arranged in concentric rings. (B) TEM micrograph (scale bar = 2 μm) showing aggregates of discrete PBs, damaged PBs (white arrows), OBs, membrane fragments and cell debris among intact PBs. (C) SEM micrograph (scale bar = 50 μm) showing mostly spherical PBs. A higher magnification (scale bar = 10 μm) (D) revealed their smooth surfaces containing occasional small pits.

the extraction procedure intact, including the acetone wash, without loss of membrane integrity. An enlarged view of a PB (Fig. 4B, inset, lower right corner) readily revealed the intensively stained periphery, implying the presence of a single membrane. Organic solvents (e.g., acetone and hexane) are often used in defatting of seeds prior to PB isolation, but they have been found unable to disrupt the membrane (Adams & Novellie, 1975; Tombs, 1967). In addition, Fig. 4B shows the electron-dense HPBs with spherical shape and homogeneous appearance. Clumps formed by aggregation of discrete PBs were also apparent, confirming our earlier LM findings. Another notable observation was the presence of disrupted PBs and membrane fragments in the sample. The white arrows point to damaged PBs, within which some solubilisation of the proteinaceous matrix had occurred, leaving behind slightly stained peripheral regions and granular amorphous materials that seemed to be the insoluble crystalloids. The membranes that appeared to have enveloped the intact PBs were still noticeable around the crystalloids. Similar TEM microstructures have been reported for PBs after contact with water or aqueous buffers (Donhowe & Peterson, 1983; Tully & Beevers, 1976). Furthermore, the TEM micrograph shows many small particles (<1 μm), presumably formed from rupture of large PBs. Interestingly, some particles possessed their own membrane-like, densely stained borders as pointed out by the red arrows. On the basis of this observation, one may infer that there apparently exists fine HPB particles corresponding to the 0.1–2 μm size fraction present in the size distribution from Fig. 3B3. The occurrence of two types of rice PBs differing in size (i.e., 1–2 μm and ~4 μm in diameter) has been described previously (Tanaka, Sugimoto, Ogawa, & Kasai, 1980). However, further research is required to ascertain whether such two kinds of PBs exist in hemp seed.

Finally, the morphology of the isolated HPBs was investigated using SEM. Fig. 4C shows large aggregates consisting of numerous spherical or elliptical particles. The majority of the particles appeared to be PBs that remained intact after the isolation and drying procedure. Higher magnification revealed two distinct fractions differing in particle size. The large fraction contained mostly intact PBs from 2 μm to more than 5 μm in diameter with spherical shape. These particles had relatively smooth regular surfaces that contained occasional small pits but were mostly free of cytoplasmic materials. The aqueous extraction used in this study could have dissolved and washed away the cytoplasmic network originally attached to their surfaces (Wolf & Baker, 1975). On the other hand, the fine fraction contained irregularly shaped, small particles <2 μm in diameter. These were likely proteinaceous granules that formed as a result of the destruction of larger PBs as mentioned above. Freeze drying used in SEM sample preparation is also known to cause reduction of the size of isolated PBs (Lee et al., 1983).

3.5. Protein composition of hemp protein fractions by SDS–PAGE

The protein profiles of the hemp milk and its various fractions obtained by centrifugation were analysed by SDS–PAGE under both

reducing and non-reducing conditions (Fig. 5). The proteins present in the hemp milk (lane HM) were resolved into >15 bands of diverse molecular weight (MW) ranging from 5 to >250 kDa. Under the non-reducing condition, the hemp milk preparation yielded prominent bands with MWs of around 48–54 kDa and 10–15 kDa. These bands were typical of the two major classes of hemp storage proteins, globulin and albumin, respectively.

Globulins (7 S and 11 S) constitute about 65–80% of the total hemp seed protein while the remaining 20–30% represents albumin (2 S). Edestin is the predominant hemp globulin, and like most 11 S globulins, is a hexamer with MW of about 320 kDa. Being a hexamer, edestin is composed of six identical subunits (monomers), each consisting of an acid α subunit (AS) and a basic β subunit (BS) linked by a disulfide bond (Potin & Saurel, 2020). The band around 54 kDa (lane HM) in the non-reducing gel was assigned to edestin monomer (AS–BS). This band disappeared when treated with the reducing agent (β-ME) due to reduction of the disulfide bond linking the two edestin subunits, releasing three distinct bands at ~34, ~21 and ~18 kDa. While the former was identified as the AS, the latter two most likely corresponded to the more heterogenous BS (Garcia et al., 2021; Potin & Saurel, 2020). In addition to the 11 S globulin (edestin), a fainter band around 48 kDa was also visible and seemed little affected by the reduction with β-ME. This band could be attributed to the characteristic subunit of the 7 S globulin (Potin, Lubbers, Husson, & Saurel, 2019). The albumin fraction of the hemp milk was resolved by non-reducing SDS–PAGE into several bands (MW 10–15 kDa). One major band was detected around 12 kDa and was replaced by two bands at <10 kDa upon the addition of β-ME. Fang, Chang, Ohm, Chen, and Rao (2023) have identified a 2 S albumin with MW of 14 kDa in hemp protein isolate. It consists of two covalently linked peptide chains that are dissociated under reducing conditions, forming a band at ~9 kDa.

Upon centrifugation, most of the protein bands detected in the hemp milk were retained in the PB pellet (lane PBP), the remaining protein was found in the supernatant (lane S). This was expected since the hemp storage proteins are mainly situated in the PBs (Angelo et al., 1968). The edestin polypeptide bands were the most intense and well-resolved on the SDS–PAGE gels of the PB pellet. This analysis suggests that globulin edestin, presumably confined within the crystalloid, is the most abundant protein component of the HPBs. Besides edestin, fainter bands (MW 10–15 kDa) corresponded to the albumin fraction that is supposedly localised in the proteinaceous matrix. Further, the PB pellet (lane PBP) and the washed HPBs (lane WPB) showed very similar SDS–PAGE patterns under both the non-reducing and reducing conditions. This observation indicates that the extensive acetone-water washing procedure did not have substantial impact on the PB composition. More specifically, the solubilisation of the crystalloid (mainly edestin) and the matrix proteins (albumins) was apparently minimal under the washing conditions used.

Unlike the PB fractions that contained proteins of diverse MW, the supernatant fraction (lane S) was composed chiefly of low MW proteins (<15 kDa). These bands, characteristic of the water-soluble albumins, were consistent with those found in the hemp milk and the isolated HPBs. It is inevitable that the aqueous media used to isolate PBs would cause, to some extent, the extraction of low MW albumins from the organelles (Higgins, 1984), resulting in their subsequent appearance in the supernatant fraction as seen in this study. Interestingly, low MW storage albumins, apart from being an integral component of the PBs, have also been found in the cytoplasm of the cotyledon cells surrounding the PB and OB organelles (Higgins et al., 1987; Manickam & Carlier, 1980; Murray, 1979). This raises questions as to whether the water-soluble albumins present in the supernatant fraction were derived mainly from proteins solubilised from the HPBs, which would guarantee further investigation.

3.6. Physicochemical characterisation

3.6.1. Effect of pH and ionic strength on electrical surface charge of hemp protein bodies

Fig. 6 presents the ζ–potential of isolated HPBs as a function of pH (2–8) and ionic strength (0, 0.01, 0.1, and 1 M NaCl) at 25 °C. The pI, the pH at which the proteins carry no net electrical charge, was estimated to be around 4.5. The typical range of pI for hemp proteins is 4.5–5, as has

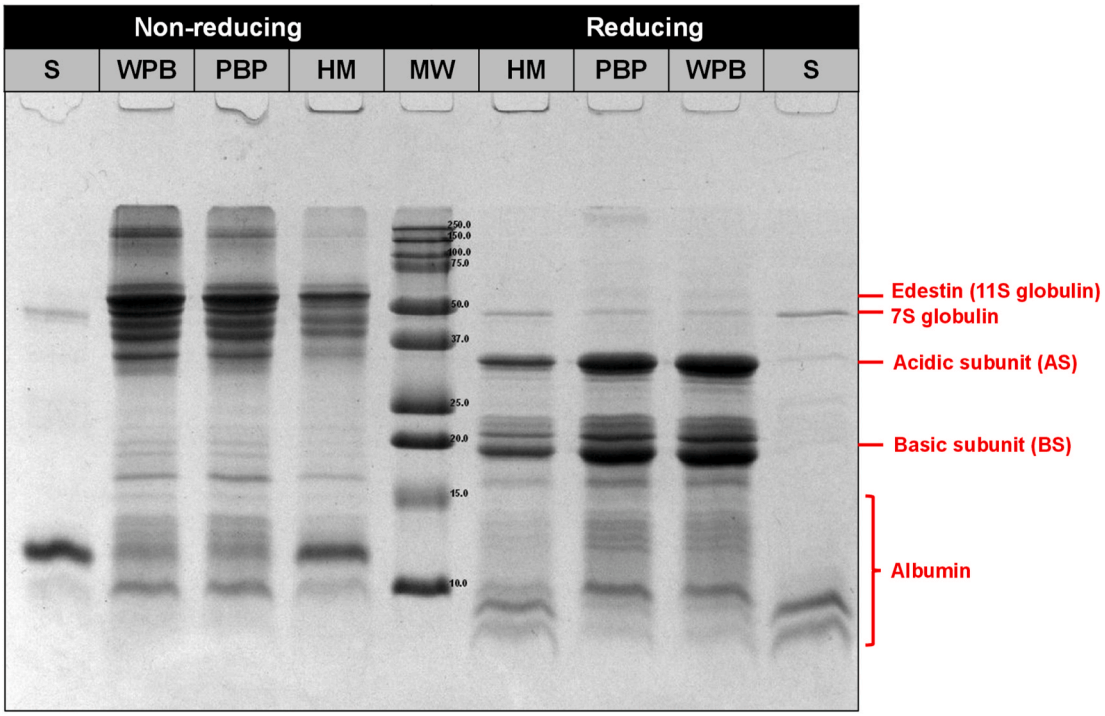

Fig. 5. SDS-PAGE profiles of hemp milk and its fractions obtained by centrifugation. The samples were prepared in reducing and non-reducing conditions. Abbreviations: MW, molecular weight marker in kDa; HM, hemp milk; PBP, protein body pellet; WBP, washed protein bodies; S, supernatant.

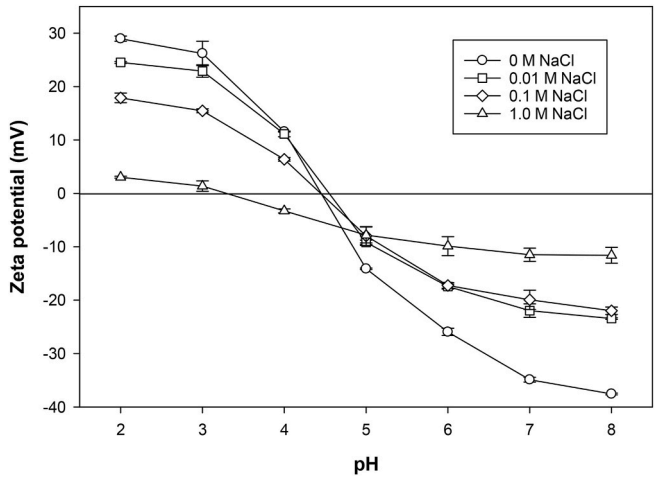

Fig. 6. Effect of pH (2–8) and ionic strength (0, 0.01, 0.1, and 1 M NaCl) on zeta potential of isolated HPBs.

been reported earlier (Ajibola & Aluko, 2022). The PB surfaces became positively charged at the pH levels below the pI due to the protonated amine groups (NH_3^+) and negatively charged above the pI due to the deprotonated carboxyl groups (COO^-). For example, at ionic strength of 0 M NaCl, the ζ-potential switched from ~29 mV at pH 2 to ~ −38 mV at pH 8.

The slope of the ζ–potential curve as a function of pH was clearly affected by ionic strength. Specifically, as the NaCl concentration increased from 0 to 1 M, the slope became progressively less steep, and the absolute value of the ζ–potential generally decreased. According to the classical DLVO theory of colloidal stability, counter ions (Na^+ and Cl^-) in solutions shield the surface charges of colloidal particles. This charge screening effect is associated with decreases in both the absolute value of the ζ–potential and the thickness of the electric double layer. Consequently, the electrostatic repulsion between the charged particles is reduced, which would promote PB–PB aggregation (Li & Xiong, 2021). Overall, the pH and ionic strength play an important role in influencing the electrostatic repulsion between HPBs due to surface charges, which will dictate their colloidal stability as we will show in the following section.

3.6.2. *Effect of pH on stability of hemp protein bodies*

The stability of isolated HPBs dispersed in water was examined through changes in their particle size (Fig. 7A) and microstructure (Fig. 7B) at various pH levels (2–13). As shown in Fig. 7A, the volume-weighted average diameter ($d_{4,3}$) over the pH range studied resembled a U–shaped curve with a trough at pH 7 and two peaks at extreme pH values.

Looking more closely at this curve, a slight downward trend of the $d_{4,3}$ was apparent in the pH 5–7 region, which could be explained by the ζ–potential data (at ionic strength of 0 M NaCl) (Fig. 6). As the pH increased from 5 (~pI) to 7 (neutral), the ζ–potential became more negative (−14.2 and −34.9 mV). This, in turn, promoted particle dissociation due to increased electrostatic repulsion between the negatively charged HPBs. These results are further corroborated by LM observations (Fig. 7B). Specifically, discrete HPBs tended to clump together at pH 5 (~pI), forming large grape-like clusters (Fig. 7B4), as evidenced by their low negative surface charges. However, the aggregation was weak and reversible. When the pH was adjusted away from the pI, the particles became somewhat less aggregated at pH 6 (Fig. 7B5), and virtually no aggregation could be observed at pH 7 (Fig. 7B6). The absolute ζ–potential at pH 7 (34.9 ± 0.5 mV) was well above 30 mV, indicating that the electrostatic repulsion dominated the van der Waal attractive forces. Accordingly, the charged particles had a strong tendency to separate from one another and exhibited high colloidal stability. Nevertheless, pH 5 appeared to confer the greatest structural stability (intactness), most likely because it is close to the pI corresponding to the minimum solubility of hemp proteins. From Fig. 7B4, little or no degradation of the HPBs was observed at pH 5. However, some large PBs started bursting at pH 6 and 7, generating small protein fragments (Fig. 7B5–6). Some studies have reported the rupture of intact PBs when they are suspended in water (neutral pH), producing numerous proteinaceous particles of less than 1 μm in diameter (Lee et al., 1983; Lui & Altschul, 1967). It is interesting to note that the $d_{4,3}$ at pH 7 (4.6 ± 0.0 μm) would reflect the true average diameter of individual HPBs rather than their aggregates. Nevertheless, the rupture of some large PBs at this pH will likely skew the distribution towards small size range (<1 μm), resulting in relatively smaller average size of isolated HPBs compared to those present in seed tissues as discussed earlier.

When the pH deviated from the pI–neutral–pH region, the $d_{4,3}$ increased sharply and reached maximum under extreme acidic (pH 2) and alkaline (pH 13) conditions. LM evidence obtained from Fig. 7B suggests that the HPBs had undergone irreversible structural transformations in both the acidic (pH 2–4) and alkaline (pH 8–13) regions. In the acidic region (Fig. 7B1–3), a large number of particles remained intact and retained their original spherical form. However, the disruption of PBs was apparent and protein molecules released from the disrupted bodies appeared to form large aggregates entrapping the remaining intact bodies. The formation of the protein aggregates caused a shift in the size distribution towards large size range, which was responsible for the observed sharp increase in the $d_{4,3}$ (Fig. 7A). Such structural changes were far more dramatic in the alkaline region.

Indeed, the HPBs were highly swollen and displayed a globular, translucent appearance at alkaline pH 8–11 (Fig. 7B7–10). Eventually they became irregular, aggregated and often fused into a single mass. At pH 12 (Fig. 7B11), some PBs swelled considerably to several times their original size but remained intact, whereas most PBs had apparently ruptured and released protein molecules into the solution. At the extreme pH 13 (Fig. 7B12), the PBs were no longer visually perceptible. Evidently, they had completely disintegrated, but were not fully dissolved. Proteins and membrane fragments released from the ruptured PBs appeared to have coalesced into large aggregates that were visible under LM. Also noticeable in Fig. 7B12 and indicated by the blue arrows is the presence of numerous small vesicles (0.1–1.0 μm), comparatively smaller in size than the PBs. These vesicles were identifiable as insoluble phytin globoids liberated from the HPBs following their dissolution (Lui & Altschul, 1967). Additionally, we observed that the HPB dispersions disintegrated virtually completely to give a clear solution at both pH 12 and 13 as opposed to turbid suspensions seen at other pH levels tested (results not shown). In line with our findings, it was reported that soybean PBs became solubilised at pH 12, and thus were not visible when viewed under an optical microscope (Lee et al., 1983).

The swelling and dissolution of HPBs under the influence of acid or alkali closely resembled that previously reported for milk protein microgel particles (Mercadé-Prieto, Falconer, Paterson, & Wilson, 2007; Sağlam, Venema, de Vries, & van der Linden, 2013). The swelling phenomenon is mainly attributed to the internal osmotic pressure arising from the ionisation of pH-responsive groups of proteins and the consequent increase in free counter ion concentration inside the particles or, equivalently, the internal electrostatic repulsion (Saunders & Vincent, 1999; Sağlam et al., 2013). Osmotic swelling generally exhibits two distinct maxima (in the acid and in the alkaline range) and a minimum (corresponding to the pI of the protein) (Lloyd, 1932). This agrees well with the swelling pH region of the HPBs identified in this study. Moreover, our results showed that the HPBs became swollen and solubilised in alkaline pH to a much greater extent than in acidic pH. In fact, strong alkali solutions could penetrate the HPBs, causing them to swell greatly due to increased inter-molecular electrostatic repulsion. This is followed by cleavage of covalent bonds (i.e., disulfide bonds), increased solubilisation and leakage of proteins from the PBs, and eventual

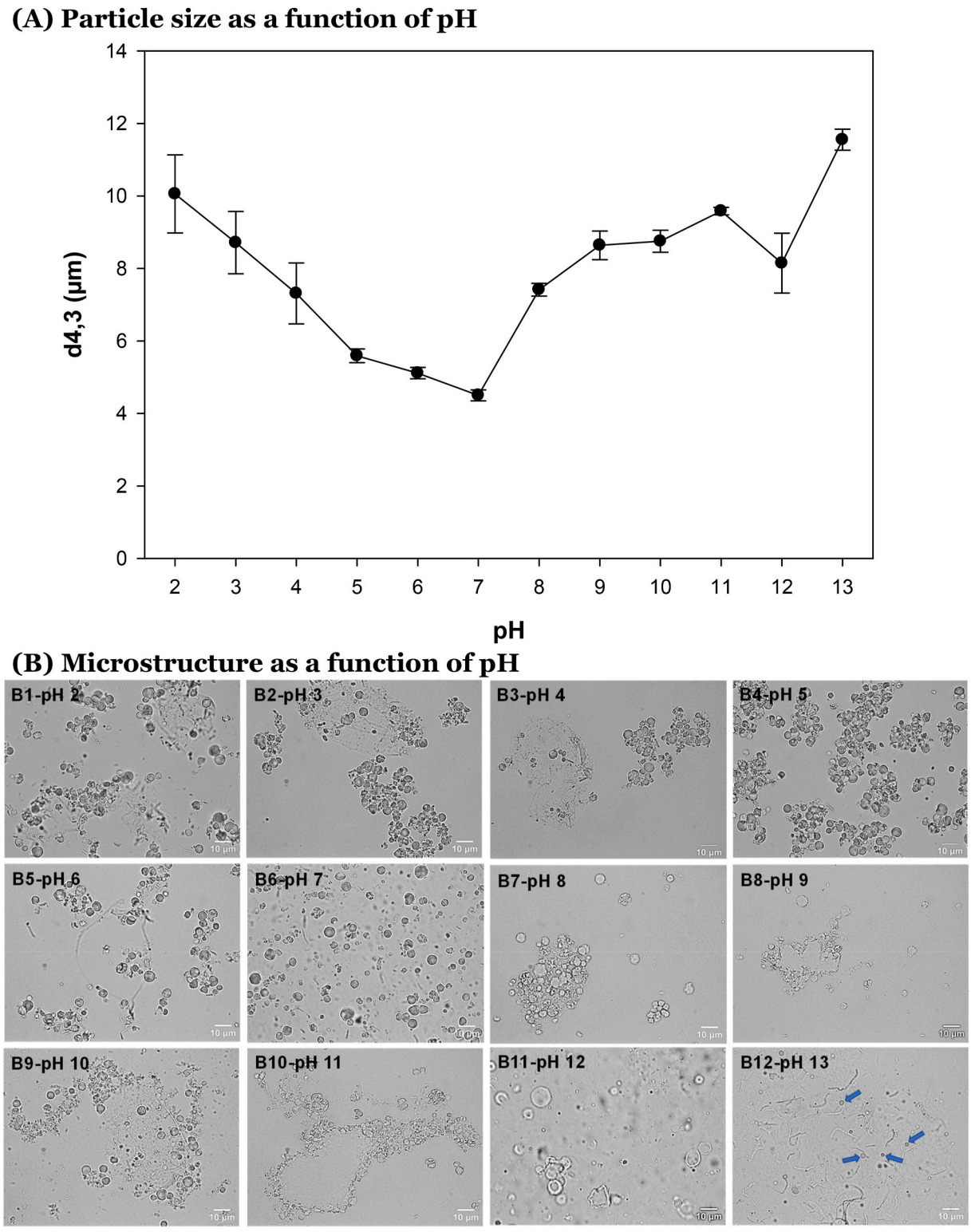

Fig. 7. Effect of pH (2–13) on volume-averaged diameter ($d_{4,3}$) (A) and microstructure (B) of isolated HPBs dispersed in water. Representative microstructural images (B1–12, scale bar = 10 μm) were taken with a light microscope (100 ×) in brightfield mode. Error bars indicate the standard deviations. Blue arrows indicate insoluble phytin globoids.

destabilization of the microstructure (Mercadé-Prieto et al., 2007; Sağlam et al., 2013). As a side note, it is interesting that the alkali-induced swelling and dissolution of the HPBs observed here is analogous to the well-known alkali gelatinisation of starch granules whereby the granules undergo extensive swelling, deformation and bursting (Wootton & Ho, 1989). In the latter case, a strong alkali solution could dissociate protons from the –OH groups and impart negative charges on the starch molecules; hence, the resulting internal electrostatic repulsion causes the starch granules to swell (Uthumporn, Shariffa, Fazilah, & Karim, 2012).

4. Conclusions

The present study has provided new insights into the isolation, microstructure, composition and physicochemical properties of HPBs. The sonication-assisted aqueous enzymatic processing applied to hemp hearts was capable of extracting a significant proportion of the intracellular PBs in their intact form. This is supported by the ultrastructural observations of the isolated organelles demonstrating that they conformed to the classic PB structure. SDS–PAGE further confirmed globulin edestin as the major component of the HPBs. However, the results also suggested some destruction of large PBs in the aqueous extraction medium, resulting in smaller size of the isolated HPBs compared to those occurring naturally in seed tissues. Therefore, various extraction conditions, e.g., aqueous versus non-aqueous media, pH, ionic strength, homogenisation, etc., must be considered when it comes to pure, intact PB preparations. Our results also provide robust evidence for the pH-responsive swelling and dissolution of the HPBs, especially in strong alkaline environments. This behaviour may modify the rheological properties of the aqueous HPB dispersions, although this point falls outside the scope of the current study. Future work will explore the possible use of the intact HPBs as a unique plant-based material for food applications. For example, these protein particles can be used to increase the protein content of foods with minimal impact on the viscosity and structure of food systems.

CRediT authorship contribution statement

Duc Toan Do: Data curation, Formal analysis, Investigation, Methodology, Validation, Visualization, Writing – original draft. **Aiqian Ye:** Methodology, Supervision, Writing – review & editing. **Harjinder Singh:** Methodology, Supervision, Writing – review & editing. **Alejandra Acevedo-Fani:** Conceptualization, Methodology, Supervision, Writing – review & editing.

Declaration of competing interest

The authors declare that the research was conducted in the absence of any commercial or financial relationships that could be construed as a potential conflict of interest.

Data availability

Data will be made available on request.

Acknowledgements

The authors thank the Riddet Institute Centre of Research Excellence (CoRE) and the Tertiary Education Commission, New Zealand, for proving funding for this research. They also acknowledge the Manawatu Microscopy and Imaging Centre (MMIC) of Massey University for providing support in data collection.

References

Adams, C. A., & Novellie, L. (1975). Composition and structure of protein bodies and spherosomes isolated from ungerminated seeds of Sorghum bicolor (Linn.) Moench. *Plant Physiology, 55*(1), 1–6.

Ajibola, C. F., & Aluko, R. E. (2022). Physicochemical and functional properties of 2s, 7s, and 11s enriched hemp seed protein fractions. *Molecules, 27*(3), 1059.

Al Loman, A., Callow, N. V., Islam, S. M., & Ju, L.-K. (2018). Single-step enzyme processing of soybeans into intact oil bodies, protein bodies and hydrolyzed carbohydrates. *Process Biochemistry, 68*, 153–164.

Alonso-Esteban, J. I., Pinela, J., Ćirić, A., Calhelha, R. C., Soković, M., Ferreira, I. C., … Sanchez-Mata, M. (2022). Chemical composition and biological activities of whole and dehulled hemp (Cannabis sativa L.) seeds. *Food Chemistry, 374*, 131754.

Angelo, A. J. S., Yatsu, L. Y., & Altschul, A. M. (1968). Isolation of edestin from aleurone grains of Cannabis sativa. *Archives of Biochemistry and Biophysics, 124*, 199–205.

Banskota, A. H., Tibbetts, S. M., Jones, A., Stefanova, R., & Behnke, J. (2022). Biochemical characterization and in vitro digestibility of protein isolates from hemp (Cannabis sativa L.) by-products for salmonid feed applications. *Molecules, 27*(15), 4794.

Boatright, W., & Kim, K. (2000). Effect of electron microscopy fixation pH on the ultrastructure of soybean protein bodies. *Journal of Agricultural and Food Chemistry, 48*(2), 302–304.

Donhowe, E. T., & Peterson, D. M. (1983). Isolation and characterization of oat aleurone and starchy endosperm protein bodies. *Plant Physiology, 71*(3), 519–523.

Do, D. T., Singh, J., Oey, I., & Singh, H. (2018). Biomimetic plant foods: Structural design and functionality. *Trends in Food Science & Technology, 82*, 46–59.

Do, D. T., Singh, J., Oey, I., & Singh, H. (2019). Modulating effect of cotyledon cell microstructure on in vitro digestion of starch in legumes. *Food Hydrocolloids, 96*, 112–122.

Do, D. T., Singh, J., Oey, I., & Singh, H. (2020). Isolated potato parenchyma cells: Physico-chemical characteristics and gastro-small intestinal digestion in vitro. *Food Hydrocolloids, 108*, Article 105972.

DuBois, M., Gilles, K. A., Hamilton, J. K., Rebers, P. A., & Smith, F. (1956). Colorimetric method for determination of sugars and related substances. *Analytical Chemistry, 28*(3), 350–356.

Elpidina, E., Dunaevsky, Y., & Belozersky, M. (1990). Protein bodies from buckwheat seed cotyledons: Isolation and characteristics. *Journal of Experimental Botany, 41*(8), 969–977.

Fang, B., Chang, L., Ohm, J.-B., Chen, B., & Rao, J. (2023). Structural, functional properties, and volatile profile of hemp protein isolate as affected by extraction method: Alkaline extraction–isoelectric precipitation vs salt extraction. *Food Chemistry, 405*, Article 135001.

Garcia, F. L., Ma, S., Dave, A., & Acevedo-Fani, A. (2021). Structural and physicochemical characteristics of oil bodies from hemp seeds (Cannabis sativa L.). *Foods, 10*(12), 2930.

Higgins, T. (1984). Synthesis and regulation of major proteins in seeds. *Annual Review of Plant Physiology, 35*(1), 191–221.

Higgins, T. J., Beach, L. R., Spencer, D., Chandler, P. M., Randall, P. J., Blagrove, R. J., et al. (1987). cDNA and protein sequence of a major pea seed albumin (PA 2: M r≈ 26 000). *Plant Molecular Biology, 8*, 37–45.

Huang, A. H. C. (1985). Protein bodies. In H.-F. Linskens, & J. F. Jackson (Eds.), *Cell components* (pp. 134–144). Berlin, Heidelberg: Springer Berlin Heidelberg.

Krishnan, H. B. (2008). Preparative procedures markedly influence the appearance and structural integrity of protein storage vacuoles in soybean seeds. *Journal of Agricultural and Food Chemistry, 56*(9), 2907–2912.

Lee, N. Y., Kim, D. M., & Kim, E. S. (2011). Morphological study of storage granules of cotyledon cells in Cannabis sativa cv. Chungsam. *Applied Microscopy, 41*(1), 61–67.

Lee, C. H., Kim, C. S., & Yang, H. C. (1983). Microstructure and hydrodynamic properties of soybean protein bodies in solutions. *Journal of Food Science, 48*(3), 695–702.

Lending, C., Kriz, A., Larkins, B., & Bracker, C. (1988). Structure of maize protein bodies and immunocytochemical localization of zeins. *Protoplasma, 143*, 51–62.

Li, R., & Xiong, Y. L. (2021). Sensitivity of oat protein solubility to changing ionic strength and pH. *Journal of Food Science, 86*(1), 78–85.

Lloyd, D. J. (1932). The pH stability region of proteins and osmotic swelling. *Nature, 130*(3270), 24–25.

Lopez, C., Novales, B., Rabesona, H., Weber, M., Chardot, T., & Anton, M. (2021). Deciphering the properties of hemp seed oil bodies for food applications: Lipid composition, microstructure, surface properties and physical stability. *Food Research International, 150*, Article 110759.

Lott, J., & Buttrose, M. (1978). Globoids in protein bodies of legume seed cotyledons. *Functional Plant Biology, 5*(1), 89–111.

Lott, J. N., Larsen, P. L., & Darley, J. J. (1971). Protein bodies from the cotyledons of Cucurbita maxima. *Canadian Journal of Botany, 49*(10), 1777–1782.

Lui, N. S. T., & Altschul, A. M. (1967). Isolation of globoids from cottonseed aleurone grain. *Archives of Biochemistry and Biophysics, 121*(3), 678–684.

Manderson, G., Hardman, M., & Creamer, L. (1998). Effect of heat treatment on the conformation and aggregation of β-lactoglobulin A, B, and C. *Journal of Agricultural and Food Chemistry, 46*(12), 5052–5061.

Manickam, A., & Carlier, A. R. (1980). Isolation and function of a low molecular weight protein of mung bean embryonic axes. *Planta, 149*, 234–240.

McClements, D. J., & Grossmann, L. (2022). The rise of plant-based foods. In *Next-generation plant-based foods: Design, production, and properties* (pp. 1–21). Springer.

Mercadé-Prieto, R., Falconer, R. J., Paterson, W. R., & Wilson, D. I. (2007). Swelling and dissolution of β-lactoglobulin gels in alkali. *Biomacromolecules, 8*(2), 469–476.

Mitsuda, H., Murakami, K., Kusano, T., & Yasumoto, K. (1969). Fine structure of protein bodies isolated from rice endosperm. *Archives of Biochemistry and Biophysics, 130*, 678–680.

Müntz, K. (1998). Deposition of storage proteins. *Protein Trafficking in Plant Cells*, 77–99.

Murray, D. R. (1979). A storage role for albumins in pea cotyledons. *Plant, Cell and Environment, 2*(3), 221–226.

Pernollet, J.-C. (1978). Protein bodies of seeds: Ultrastructure, biochemistry, biosynthesis and degradation. *Phytochemistry, 17*(9), 1473–1480.

Potin, F., Lubbers, S., Husson, F., & Saurel, R. (2019). Hemp (Cannabis sativa L.) protein extraction conditions affect extraction yield and protein quality. *Journal of Food Science, 84*(12), 3682–3690.

Potin, F., & Saurel, R. (2020). Hemp seed as a source of food proteins. In G. Crini, & E. Lichtfouse (Eds.), *Sustainable agriculture reviews 42: Hemp production and applications* (pp. 265–294). Springer.

Prattley, C. A., & Stanley, D. (1982). Protein-phytate interactions in soybeans. I. Localization of phytate in protein bodies and globoids. *Journal of Food Biochemistry, 6*(4), 243–254.

Sağlam, D., Venema, P., de Vries, R., & van der Linden, E. (2013). The influence of pH and ionic strength on the swelling of dense protein particles. *Soft Matter, 9*(18), 4598–4606.
Saunders, B. R., & Vincent, B. (1999). Microgel particles as model colloids: Theory, properties and applications. *Advances in Colloid and Interface Science, 80*(1), 1–25.
Shen, P., Gao, Z., Fang, B., Rao, J., & Chen, B. (2021). Ferreting out the secrets of industrial hemp protein as emerging functional food ingredients. *Trends in Food Science & Technology, 112*, 1–15.
Tanaka, K., Sugimoto, T., Ogawa, M., & Kasai, Z. (1980). Isolation and characterization of two types of protein bodies in the rice endosperm. *Agricultural and Biological Chemistry, 44*(7), 1633–1639.
Tombs, M. (1967). Protein bodies of the soybean. *Plant Physiology, 42*(6), 797–813.
Tully, R. E., & Beevers, H. (1976). Protein bodies of castor bean endosperm: Isolation, fractionation, and the characterization of protein components. *Plant Physiology, 58*(6), 710–716.
Uthumporn, U., Shariffa, Y., Fazilah, A., & Karim, A. (2012). Effects of NaOH treatment of cereal starch granules on the extent of granular starch hydrolysis. *Colloid and Polymer Science, 290*, 1481–1491.
Varriano-Marston, E., & DeFrancisco, A. (1984). Ultrastructure of quinoa fruit (Chenopodium quinoa Willd). *Food Structure, 3*(2), 9.
Wolf, W. J., & Baker, F. L. (1975). Scanning electron microscopy of soybeans, soy flours, protein concentrates, and protein isolates. *Cereal Chemistry, 52*(3), 387–396.
Wootton, M., & Ho, P. (1989). Alkali gelatinisation of wheat starch. *Starch, 41*(7), 261–265.
Zhu, X., Ye, A., Verrier, T., & Singh, H. (2013). Free fatty acid profiles of emulsified lipids during in vitro digestion with pancreatic lipase. *Food Chemistry, 139*(1–4), 398–404.